RAL-TR-2007-003

THE HOTWAXS DETECTOR

J.E.Bateman[a], G.E.Derbyshire[a], G.Diakun[b], D.M.Duxbury[a], J.P.A.Fairclough[c], I.Harvey[b], W.I.Helsby[b], J.D.Lipp[a], A.S.Marsh[a], J.Salisbury[a], G.Sankar[d], E.J.Spill[a], R.Stephenson[a] and N.J.Terrill[e]

[a]Science and Technology Facilities Council, Rutherford Appleton Laboratory, Harwell Science and Innovation Campus, Didcot, Oxfordshire, OX11 0QX, U.K.
[b]Science and Technology Facilities Council, Daresbury Laboratory, Keckwick Lane, Daresbury, Warrington, WA4 4AD, UK
[c]Dept of Chemistry, University of Sheffield, Brook Hill, Sheffield, S3 7HF, UK
[d]Royal Institution of GB, 21 Albemarle Street, London W1S 4BS
[e]Diamond Light Source LTD, Harwell Science and Innovation Campus, Diamond House, Chilton, Didcot, Oxfordshire, OX11 0DE

14 May 2007

Abstract

The development and testing of the HOTWAXS position sensitive X-ray detector for Synchrotron Radiation Sources is described. Funded from a facility development grant, the aim of the project was to produce a high counting rate, parallax free photon counting detector to be used in the combined studies of X-ray absorption fine structure and X-ray diffraction (XAFS/XRD), and also in the technique of small angle and wide angle X-ray scattering (SAXS/WAXS). The detector system is described together with results of experiments carried out at the Daresbury Laboratory Synchrotron Radiation Source (SRS).

1. Introduction

The intense beams of X-rays afforded by synchrotron sources such as the SRS at Daresbury and Diamond at RAL, put severe demands on the associated detector technologies used to instrument the beamlines at these sources, requiring detectors which are capable of very high counting rates. For X-ray crystallographic studies involving scattering and/or diffraction in the wide angular range (5-65^o), further requirements of good spatial (i.e. angular) resolution and parallax free detection compound the issue further. A detector to match these criteria was proposed based on the Microstrip Gas Detector (MSGC) [1] which we call the High Overall Throughput Wide Angle X-ray Scattering detector (HOTWAXS).

MSGC's have been developed over many years at various centres for applications in particle physics (see for example [2]) and meet many of the demands of X-ray counting in SRS beams. Operation has been demonstrated at count rates of up to 1MHz/mm^2 of plate [3] with useful counter lifetimes corresponding to months of continuous running at these rates [4]. The geometric flexibility of the MSGC permits a one-dimensionally sensitive detector to be fabricated in which the anode strips are made to point at the sample position while the X-ray-induced electron clouds are drifted only a short distance (see reference [5] for a similar proposal), thus giving an active detection region of 50mm along each anode length.

The technical specification for the detector called for the following to be met:

- an angular range of 60^o (from 5^o to 65^o with direct beam at 0^o)
- angular resolution of less than or equal to 0.16^o (FWHM)
- a local count rate (each instrumented channel) of 1×10^6 counts per second
- a global count rate of 500×10^6 counts per second
- a uniformity of x-ray response over the detector aperture of <5%RMS
- 512 individually instrumented channels of preamplifier, discriminator and scaler

2. Detector Design

The HOTWAXS detector consists of 8 gas microstrip detector modules located on a precision mounting plate which can be seen in figure 1. Each module subtends 7.5^o with an electrode design that points to a sample position some 400mm away giving a complete angular range of 60^o. This mounting plate is bolted to a bulkhead plate, which together with the detector body and window, forms the gas envelope. A graded drift plane placed above the detector modules, within the gas volume, defines the active region of the detector. X-rays enter the gas volume through a window, parallel to the plate surface, where they interact with the gas. The electrons formed in the gas then drift down to the

plate surface where avalanche multiplication takes place and induces a pulse on the MSGC anodes.

2.1 The MSGC module

The HOTWAXS MSGC's are of the 'pointing anode' design described previously [6], thus offering a parallax free geometry. Each glass plate consists of 128 anodes of 10μm width and 50mm in active length. These are interleaved with cathodes of varying width on a pitch of 409μm at a radius of 400mm, to 460μm at a radius of 450mm and are produced in a chrome process at IMT [7] on Schott S8900 conducting glass [8]. They are designed such that two plates can be mounted beside each other with no dead region in the angular coverage, achieved by utilising a 'half cathode' on both edges of the plate and by the precision mounting of the modules. The plates themselves are glued to a printed circuit board (PCB) which offers mechanical support and are ultrasonically wire bonded to pads on the PCB which are tracked to two JAE 70 pin connectors [9]. The PCB is then glued to a precision mounting block while being accurately located in an assembly jig. The signals from the 70 way connectors are then fed, via a flexi-rigid feed-through flange, out of the gas volume to charge sensitive preamplifiers in an electronic housing.

2.2 Graded drift

A very important aspect to the design of this detector, is that of parallax free detection. As mentioned above, the plate is designed to point at a sample position to overcome these effects, but the nature of a non-uniform electrode structure introduces non-uniformities in the gain of the MSGC along the strip length. Previous work has shown that this non-uniformity can be minimised by carefully grading the anode-cathode gap width with the pitch of the tracks [10] and by using the empirically determined formula given in [6]:

$$G = \alpha P + \beta G_o$$

where G is the anode cathode gap width, G_o is the anode cathode gap at the greatest radius of curvature and P is the pitch. We obtain a variation in gain of 15% along the anode length, see figure 2. This radial gain variation can be removed further by the use of a graded drift electrode [6], which reduces the variation to 2%, see figure 1. When a ^{55}Fe source is collimated and directed parallel to the strips, the resulting pulse height distribution from the sum of eight anodes connected together, gives a FWHM energy resolution decrease from 17.3% for the case with no graded drift, to 14.3% for the case with the graded drift, see figure 3. The range of potential applied to the drift to achieve this was –3000V to –4200V for an 18mm drift depth.

Results from the prototype detector for HOTWAXS [11] also highlighted two other areas where careful attention to the drift space geometry and field pattern would benefit the detection properties of the HOTWAXS detector. These were a re-entrant window and some side field-shaping electrodes. The re-entrant window was needed in

order to remove the dead space between the X-ray transparent gas window and the beginning of the active detection region and it was found that keeping this window at the midpoint potential between drift plane and plate gave the best results. The side electrode was introduced to minimise edge field effects. A simple single electrode design proved to be unsuitable, so a piece of S8900 glass, connected to the drift plane at each grading and to a terminal at the MSGC end, proved to be more than adequate, with careful biasing.

2.3 Gas delivery system

It is a well known fact that all gas avalanche detectors are susceptible to premature ageing under intense illumination. Thus a separate program of work was undertaken to investigate this problem but will not be reported here [12]. The choice of operating gas and the materials within the gas housing can all affect the detectors lifetime and this work concluded that a mixture of 83% argon with 17% dimethylether (DME) as quencher gave a satisfactory lifetime. During these tests, MSGC detectors were exposed to illumination rates greater than 5×10^5 counts per second in an area of $1mm^2$. The detector gain at the illumination spot was periodically measured at a much reduced rate, and a gain loss of 6% was observed for an accumulated charge of 500mC/cm (equivalent to 60 days continuous high rate operation). All the materials used in the construction of HOTWAXS were tested to an anode load of 100mC/cm of charge in a test detector before being incorporated into the design. The gas distribution rig itself has also been tested and found to be acceptable, and consists of three Brookes flow meters [13] connected to a mixing manifold with snap fittings to connect to the gas cylinders and to the detector. The detector vessel was also helium leak tested and found to give a leak rate consistent with that from the O-rings of the vessel.

2.4 Detector modularity

The modularity of the HOTWAXS system gives the flexibility of individually testing each MSGC module before installation within the HOTWAXS detector housing. A test box was constructed to facilitate this with the same feed-through flexi, motherboard and preamps as would be used in the final design. A standard Ortec preamp/post amplifier combination was used to measure the gas gain of the MSGC plate using the signals from an ^{55}Fe X-ray source. To obviate the effects of diffusion spreading, signals from four neighbouring channels were fed into this chain. The gain curves obtained are shown in figure 4. The gain uniformity over a module was thus measured by effectively averaging over groups of four neighbouring channels. Figure 5 shows the variation of the gain and sigma (standard deviation) of the pulse height distribution across a full module. As can be seen in the figure, the majority of the data obtained is very uniform but both ends of the module give anomalous results due to the discontinuity in the drift field in the test rig. In the complete detector, each module is butted to a neighbouring module, which maintains a uniform drift field, except at the two outer ends of the whole detector where the edge field correctors negate this effect. If we ignore the end points, the residual variation in gain and sigma is of the order of 1%, confirming that the gas gain is very uniform over the whole plate area.

2.5 Electronic readout performance

The signals from the anodes of the MSGC modules are transmitted, via a flexi-rigid feed-through, to low noise 16 channel charge sensitive preamplifier cards (designed at RAL) located in the electronic housing which is to the rear of the bulkhead plate, as can be seen in figure 1. Eight of these preamp cards are grouped together on a mother board, which is duplicated four times around the detector. The motherboard is laid out such that two anode signals are fed to the input of one channel of preamp. Thus we have 1024 anodes instrumented with 512 individual readout channels, with each channel consuming approximately 50mW of power. The differential voltage pulse produced by this preamp is fed, via a kapton flexi-rigid to a 70 pin D-type bulkhead connector. These differential outputs are then sent via a 15m cable to remote discriminator cards housed in a VME crate, where the signals are processed further. The discriminator boards (also designed at RAL) can be programmed to gain normalise the signals and to adjust the DC offsets of all channels independently. The boards also have the capability to base line restore and to sum neighbours, though we have the ability to fully disable both functions. To achieve the high frame rates required for time resolved experiments the signals from the discriminators are fed to 32 bit scalers housed in a further VME crate. These scalers are built on the Generic Data Acquisition (GDAQ) cards, which have previously been developed and which are already in use on the RAPID systems [14]. A time frame generator, type EC470 [15], controls the GDAQ modules ensuring the capability to frame the data down to a minimum of 10μs per frame, with a 10μs dead frame (using a double buffering technique). A large quantity of inbuilt memory is used to locally store the scaler data before the card must be readout to a PC.

Each assembled MSGC block was tested in the test box, using a unit of the 16 channel preamp readout. Figure 6 shows the corresponding pulse heights obtained for ^{55}Fe uncollimated illumination from two modules, ignoring the 4 end channels from either side. Each module is tested in this way and the results from the measurement of 10 modules recorded. This process stretched over a considerable period leading to inevitable global gain shifts from the changes in ambient conditions (pressure and temperature). Accordingly the results from two modules measured under similar ambient conditions (nos. 15 and 17) are presented in figure 6. Apart from the slight upward concavity of the pulse height at the module ends due to the drift field distortion (see above), there is a clear common mode in the fluctuations of the pulse height in the two modules. This variation is almost certainly due to component tolerances on the preamplifier (which can be removed with the discriminator gain control) and can be removed by simply ratioing the two curves to produce the third plot in figure 6. Thus we see the 4% RMS fluctuations in the raw plots reduced to 2.12% (the outlier in channel 30 is omitted). Histogramming these residuals gives a normal distribution indicating that this is the stochastic limit of the various irreducible noise factors. The difference between these two figures is about 3.5% and is compatible with the channel to channel fluctuations in the readout electronics – as noted above, provision is made to adjust the channels electronically and minimise this contribution.

3. System performance

The HOTWAXS detector and associated readout electronics were taken to the SRS and installed successively on target station 16.1, which is on a fixed wavelength beamline of 1.41Å (8.79keV) [16], and the materials science station 9.3, which is tuneable in the energy range 6-30keV [17]. A series of systematic tests have been undertaken with the system, which will be discussed in detail. As an example of the overall detector performance, the diffraction pattern obtained (at an X-ray energy of 7.6keV) from a sample of the aluminophosphate CoAlPO 34, typical of the type under study on 9.3, is shown in figure 7. It should be noted that seven dead channels have been interpolated in the figure and several less serious glitches in the response are observed (see below for discussion).

3.1 Spatial (angular) resolution

A primary requirement for crystallographic applications is a good spatial (i.e. angular) resolution. The angular resolution delivered by the detector is determined by the spatial resolution (in the θ direction) realised for an x-ray interaction in the detector convolved with the profile of the primary beam-sample interaction spread. Within the detector an ultimate limit to the spatial resolution is set by several factors, notably the photoelectron ranges, (see for example, the measurements of Smith et. al. [18]) the diffusive spread of the secondary electron cloud as it travels to the anode and the statistical and electronic noises. (A systematic study of these processes is presented in ref.[19]). The large finite depth of gas counters means that geometric limitations are also very significant. The pointing nature of the MSGC geometry removes parallax in the θ direction but imposes careful alignment requirements. Fiducial marks on the detector vessel and alignment jigs have been manufactured to ensure that the sample is placed at the detector 'focus'. Measurements have shown that if the sample is placed 10mm further from the detector than the sample position that the measured resolution increases by 2%, and if the sample is 10mm closer to the detector than the sample position then the resolution increases by 20%. Parallax limitations due to the sagittal error in the drift direction (18mm depth) only become significant at low scattering angles (θ <10 degrees)

In order to measure the spatial resolution of the detector a series of measurements were performed on station 9.3 with a rotating silicon sample. Data were obtained at X-ray energies of 8, 10, 12, 14, 16, 18, 20, 22 and 24keV in both an argon DME gas mixture and a xenon DME gas mixture (of ratio 83:17, i.e. with 83% of noble gas). Figure 8 shows the scattering data at the energies 10keV and 24keV for both the argon and xenon mixture. The second order peak (at ~ channel 291 for the 10keV case in figure 8) was used for further analysis, and a Gaussian fit to this peak at each X-ray energy was performed for both the argon and xenon based gas mixtures. The value of sigma obtained from the fit is related to the FWHM by simply multiplying by 2.35. Figure 9 shows how the experimentally fitted FWHMs vary with X-ray energy over the range. The angular resolution in figure 9 is exact but a mean strip width (0.85mm) is assumed for the spatial result. The graph also shows a comparative set of data which has been obtained from a Montecarlo simulation of this type of detector [20]. The parameters adopted in the model

did not correspond to those used experimentally so some discrepancy is inevitable. The model showed that the channel discriminator setting determines (strongly) the trade-off between spatial resolution and detection efficiency and that the optimum setting is around 50% of the total X-ray signal deposit. In the experimental case, the threshold is fixed and low leading to a slightly higher resolution than predicted and a much more rapidly increasing FWHM as the X-ray energy rises. Comparison of the experimental and modelling results for argon in figure 9 clearly show this effect.

3.2 Detector uniformity

The uniformity of the detector's response is critical when looking at systems where the angle of diffraction/scattering features can change. The usual method of flooding the detector with a remote ^{55}Fe source would not yield adequate statistics so an alternative was found in the smooth distribution at the detector by air scatter of the SRS X-ray beam (figure 10). A smooth distribution such as the air scatter can be fitted to any desired degree of accuracy with a piecewise polynomial fit. Figure 10 shows this to be the case and displays the residuals for the fit as a function of readout channel. If one ignores the glitches (see below) the detector shows a uniformity <2% RMS (typically 1.7%) over almost 75% of its aperture. This is very satisfactory. However, the very obvious glitches in the response spoil this picture. They are attributed to a major problem experienced with the flexi-rigid connectors which have been found to be prone to track breakage. There are two sets of connectors in each signal path – between the detector and the preamplifiers and between the post-amplifiers and the SCSI connectors. A failure in the second set leads to a complete loss of signal and the seven dead channels mentioned above. A failure in the first set is not so catastrophic because of the summing of two channels into one preamplifier. In this case all signal is not lost and a glitch results. Most modules seem to suffer only the one or two breakages; however, module no.7 is particularly bad. When the connection problems are rectified, the global uniformity should be a very satisfactory sub 2%.

As figure 7 shows, many X-ray lines of interest produce peaks which are of the order of the strip width. It is thus important to check that the sampling involved does not compromise the measurement of line intensity in these cases. In order to evaluate this effect the detector was attached to a mount which had the ability to rotate about the sample position. A silicon sample was illuminated and the detector was manually moved through approximately 20^{o}. The diffraction data was recorded at a variety of small steps in angle. A typical spectrum can be seen in figure 11. The boundaries between modules were of particular interest as we rely on the tolerances of the module support plate to accurately locate neighbouring modules. Each diffraction order was analysed and figure 12 shows how the peak counts and integral counts under a Gaussian fit to the data for the 4^{th} order vary as the diffraction peak moves across the detector. The variation of sigma is also shown. A residual variation of 4% RMS for the integral and peak counts is obtained and the measured peak width (σ in channels) has a variation 8% RMS. The module boundary at channel 128 is not noticeably different from the rest of the module. Closely spaced scanning across channels 151 – 154 shows no increase in the scatter of results as the X-ray peak crosses the channel boundaries.

3.3 Detector efficiency

The detection efficiency of HOTWAXS is primarily set by the active interaction depth of 50mm and its noble gas filling. This sets a theoretical limit to what efficiency can be achieved for the particular choice of gas filling (argon or xenon). In addition there are losses from the absorption of the window and any dead spaces within the front of the counter, though every engineering effort has been made to minimise these. Whilst an absolute measurement of the detection efficiency was not possible as there were too many unmeasured energy dependent variables wrapped into the calculation, the data described in section 3.1 has been used to give an estimate of the total system response over the energy range 8-24keV. Again the second order peak (at ~ channel 291 for the 10keV case in figure 8) was used for further analysis, and Gaussian fits to this peak for each X-ray energy were performed for both the argon and xenon based gas mixtures to obtain peak intensity values. From this we obtain the energy response curves shown in figure 13. This figure also shows the ratio between the xenon and argon response curves (corrected for beam decay) along with the theoretical ratio of absorption between xenon and argon. The agreement between the measured and calculated ratios is reasonably good because all the external energy dependent terms are the same in both cases. Residual effects such as the differential readout efficiency to be expected from the two gases (as predicted by the Montecarlo model [20]) probably explain the discrepancy between the data and the simple calculation of efficiency used for the ratio curve.

3.4 Counting rate performance

Strongly scattering samples were used on beam station 16.1, in order to investigate the counting capabilities of the detector. A sample of high density polyethylene (HDPE) gives two bright peaks in the angular range covered by HOTWAXS (from the 110 and 200 reflections). The detector was moved to be in a position where the horizontal straight through beam was lined up on the centre of the detector (i.e. between modules 4 and 5). A lead beam stop was positioned to absorb the direct beam. In this position the detector accepted diffraction data in an approximately $\pm 30^{o}$ range. With the HDPE sample mounted diffraction data were taken and one half of the detector had various thicknesses of attenuator covering the entrance window. Figure 14 shows the data when 10 attenuating sheets are covering half of the detector window with no attenuators present on the other half. The figure highlights the dynamic range of the detector with six orders of magnitude present on the detector at the same time. The scattering peaks numbered 1-3 have been analysed using a Gaussian fit with a constant background term. For each of the scattered peaks, the unattenuated rate is normalised to the case with the largest attenuation (where the deadtime correction is negligible) and scaled to obtain an estimated input rate for subsequent measurements. Figure 15 shows this data and a fit to the standard pile-up formula gives a deadtime value of 350ns which is smooth and reproducible. In this detector the deadtime is a property of each channel (not of the whole counter) and any correction must be applied to each channel. The smooth fit in figure 15, derived as it is from a selection of different channels shows that

the tolerance on the timing performance of the electronics is tight and a single correction curve can be applied to all channels, thus simplifying processing.

Figure 15 shows that a deadtime correction should be applied to any data taken where the peak counting rate in any single channel exceeds 1×10^5 counts per second. Figure 16 shows deadtime corrected HDPE diffraction data compared to the case with no deadtime correction (again the 7 dead channels have been interpolated in the data). The local count rate on the peak channel of the 110 reflection is increased from 1.03×10^6 to 1.62×10^6 counts per second and the global count rate is increased from 27×10^6 to 30×10^6 counts per second. The angular resolution is also slightly enhanced from 0.301^o with no correction to 0.263^o for the deadtime corrected data.

The performance of HOTWAXS should ideally be compared to the detector described in [5] which is in use at the DUBBLE beamline at the ESRF, but unfortunately we have insufficient data to do this. The RAPID2 detector which is also a wide angle, parallax free, gas based, photon counting detector, based on wire technology, has separately been compared to the DUBBLE detector [21]. A comparison between the performance of HOTWAXS and RAPID2 proved to be possible and was duly performed. The RAPID2 detector inevitably has a superior spatial resolution (compared to HOTWAXS) due to the nature of its interpolative readout method. It also possesses a similar local count rate performance but the global count rate is limited to ~ 40×10^6 counts per second by the readout method. Whilst this may not be a problem currently, for more intense sources this may be a limiting issue. Figure 17 shows HDPE scattering data on beam target station 16.1 with HOTWAXS, and from station 6.2 with RAPID2. The RAPID2 readout range of 1024 channels has been compressed by a factor of 2 in order to be plotted on the same scale. The improved angular resolution with RAPID2 is immediately apparent, as is the lower background (due to the use of an evacuated nose cone), however the global count rate from RAPID2 is ~ 3 times less at 12×10^6 counts per second, compared to 30×10^6 counts per second. The rate in the 1^{st} order peak is also greater in HOTWAXS (4.1MHz) compared with the RAPID2 peak (1.6MHz) though it should be noted that the HOTWAXS data is slightly inflated with double counts.

4. Application to time resolved diffraction studies

HOTWAXS has primarily been designed and built to collect time resolved XRD and WAXS data (in combination with either XAFS or SAXS). This is achieved by using a time frame generator (as described in 2.5) to control the scalers; the frame length and number of frames are set in the software. In order to study fast chemical changes within the sample under study, it may be necessary to collect data at the microsecond level. Figure 18 shows diffraction data obtained from HOTWAXS (from a HDPE sample on station 16.1 of the SRS) with varying time frame periods. The figure shows that the two main scattering peaks can be clearly seen with a time frame period of 100μs. To collect data at smaller time intervals than this would probably require the use of a more intense machine.

A standard WAXS phase change experiment was performed by melting and re-crystallising HDPE. The sample temperature was ramped from 120°C to 150°C at a rate of 50°C per minute, held at 150°C for one minute and was then cooled from 150°C to 120°C at 50°C per minute in a DSC on station 16.1. The material structure during the process was followed in the scattering pattern observed in HOTWAXS, with time frames of 0.3s length and with a total of 1024 frames (5 minutes in total). Figure 19 shows the data represented in 3D, but only 128 frames are shown for clarity. The phase change can clearly be observed. Solid state kinetic reactions have been studied on station 9.3 where structure evolution during high temperature zeolite collapse has been followed. The crystallisation of solids from gel mixtures has also been observed.

5. Conclusions

Based on MSGC technology with independent channel by channel readout, the HOTWAXS detector has proved itself to be an excellent WAXS detector. The detector delivers high local and global counting rate performance with acceptable parallax free angular resolution. The detector has now been commissioned on stations 2.1 and 9.3 of the SRS Daresbury, where time resolved diffraction / scattering experiments have been performed and is currently available to all users of the Daresbury Laboratory. A second, identical system is currently in production for the non crystalline diffraction beamline I22 of the Diamond synchrotron light source.

This development has been funded via the facilities development board of the Science and Technology Facilities Council.

References

1. A. Oed, Nucl. Instr. & Meth. A261(1988) 351
2. J.E. Bateman, J.F Connolly, R. Stephenson, M. Edwards and J.C. Thompson, Nucl. Instr. and Meth. A348 (1994) 372
3. R. Bouclier, M. Capeans, G. Manzin, G. Million, L. Ropelewski, F. Sauli, L.I. Shekhtman, T. Temmel, G. Della Mea, G. Maggioni and V. Rigato, CERN Report, CERN-PPE/95-37
4. J.E Bateman, J.F Connolly, Yu.N. Pestov, L.I. Shekhtman, R. Mutikainen and I. Suni, Rutherford Appleton Laboratory Report, RAL-94-114
5. V. Zhukov, F. Udo, O. Marchena, F.G. Hartjes, F.D. van der Berg, W. Bras, E. Vlieg, Nucl. Instr. & Meth. A392 (1997) 83
6. J.E. Bateman, J.F. Connolly, G.E. Derbyshire, A.S. Marsh, R. Stephenson, R.C. Farrow, W.I. Helsby, B.R. Dobson, R. Mutikainen and I. Suni, RAL-TR-1998-073
7. IMT, Greifensee, Switzerland
8. Schott Glass, Duryea, Pennsylvania, USA
9. JAE Europe, Coliseum Business Center, Riverside Way, Camberley, Surrey GU15 3YL U.K

10. ATLAS Internal Note, INDET-NO-076 (1994)
11. J.E.Bateman, J.F.Connolly, G.E.Derbyshire, D.M.Duxbury, J.Lipp, J.A.Mir, J.E. Simmons, E.J.Spill, R.Stephenson, B.R.Dobson, R.C.Farrow, W.I.Helsby, R. Mutikainen and I.Suni, Nucl. Instr. and Meth. A477 (2002) 340
12. D.Duxbury in progress
13. Brooks Instruments, Emerson Process Management, Neonstraat 3, 6718 WX Ede, Netherlands
14. R.A.Lewis, W.I.Helsby, A.O.Jones, C.J.Hall, B.Parker, J.Sheldon, P.Clifford, M.Hillon, I.Sumner, N.S.Fore, R.W.M.Jones and K.M.Roberts, Nucl. Instr. and Meth. A392(1997) 32
15. Daresbury Time Frame Generator EC740
16. N.Bliss, J.Bordas, B.D.Fell, N.W.Harris, W.I.Helsby, G.R.Mant, W.Smith, and E.Towns-Andrews, Rev. Sci. Instrum. 68 (2) (1995) 1311
17. G.Derbyshire, B.Dobson, G.N.Greaves, N.Harris, P.Mackle, P.R.Moore, K.J.Roberts, N.Allinson, J.Nicoll, S.Doyle, R.J.Oldman, Rev. Sci. Instrum. 60 (7) (1989) 1897
18. G.C.Smith, J.Fischer, V.Radeka, IEEE Trans. Nucl. Sci. NS-31, No.1, 1984, 111-115
19. J.E Bateman, Rutherford Appleton Laboratory Report, RAL-TR-2005-010
20. J.E Bateman, Rutherford Appleton Laboratory Report, RAL-TR-2006-004
21. R.J.Cernik, P.Barnes, G.Bushnell-Wye, A.J.Dent, G.P.Diakun, J.V.Flaherty, G.N.Greaves, E.L.Heely, W.I.Helsby, S.D.M.Jacques, J.Kay, T.Rayment, A.Ryan, C.C.Tang and N.J.Terrill, J. Synch. Rad., 11 (2004) 163

Figure 1: Partially assembled HOTWAXS detector showing eight MSGC modules

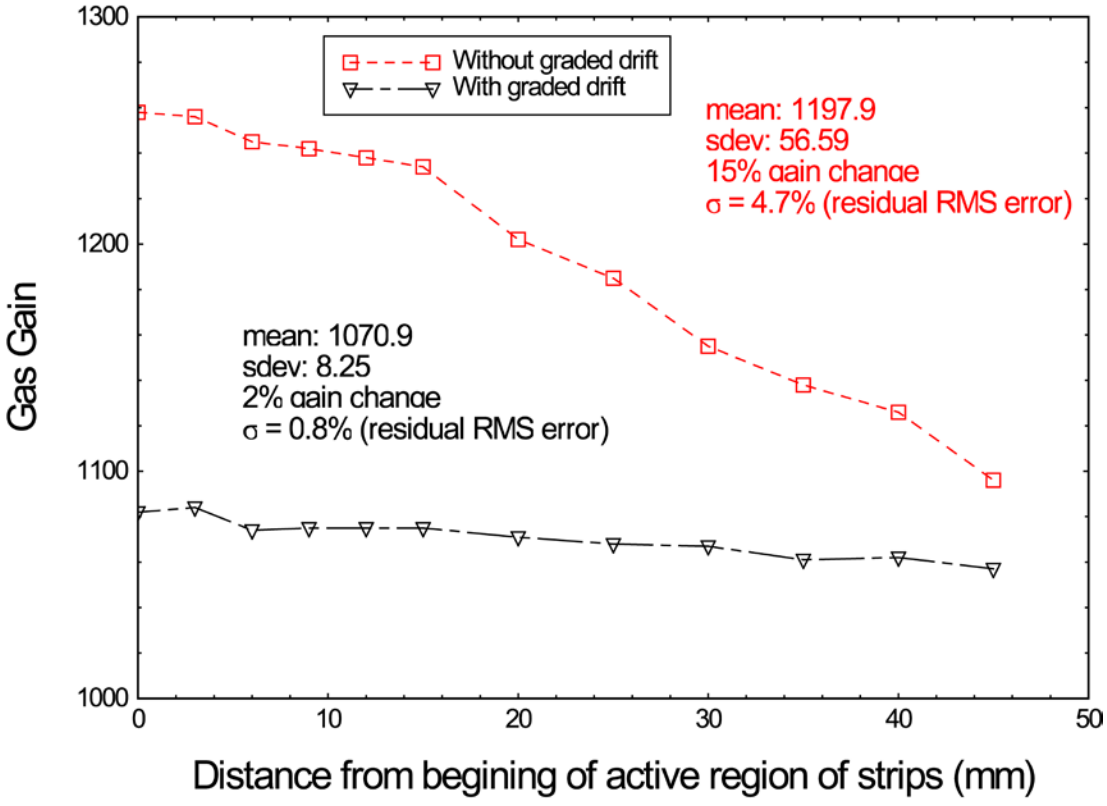

Figure 2: Measured Gas Gain variation along anode length

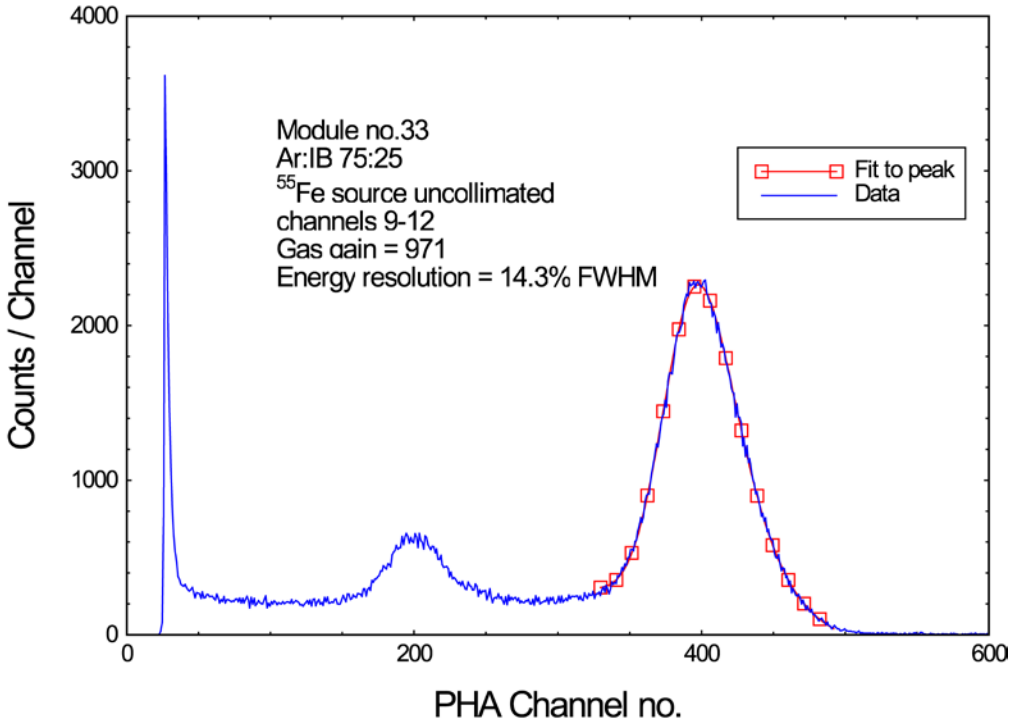

Figure 3: Typical pulse height distribution of ^{55}Fe X-rays from the sum of eight anodes with the graded drift field in place

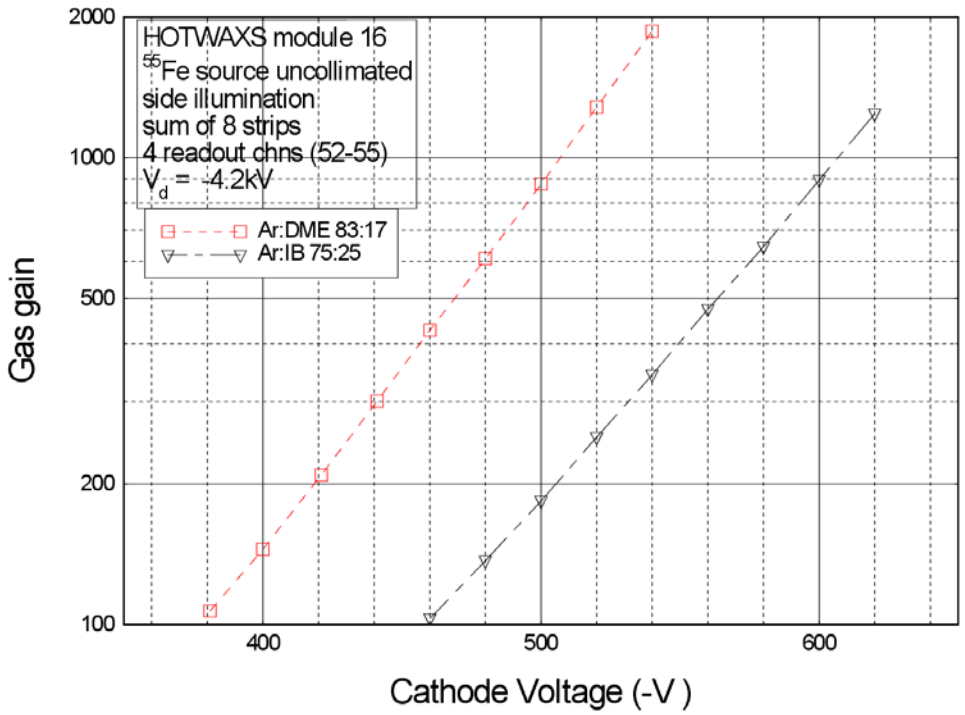

Figure 4: Gas Gain curves obtained with HOTWAXS module no.16

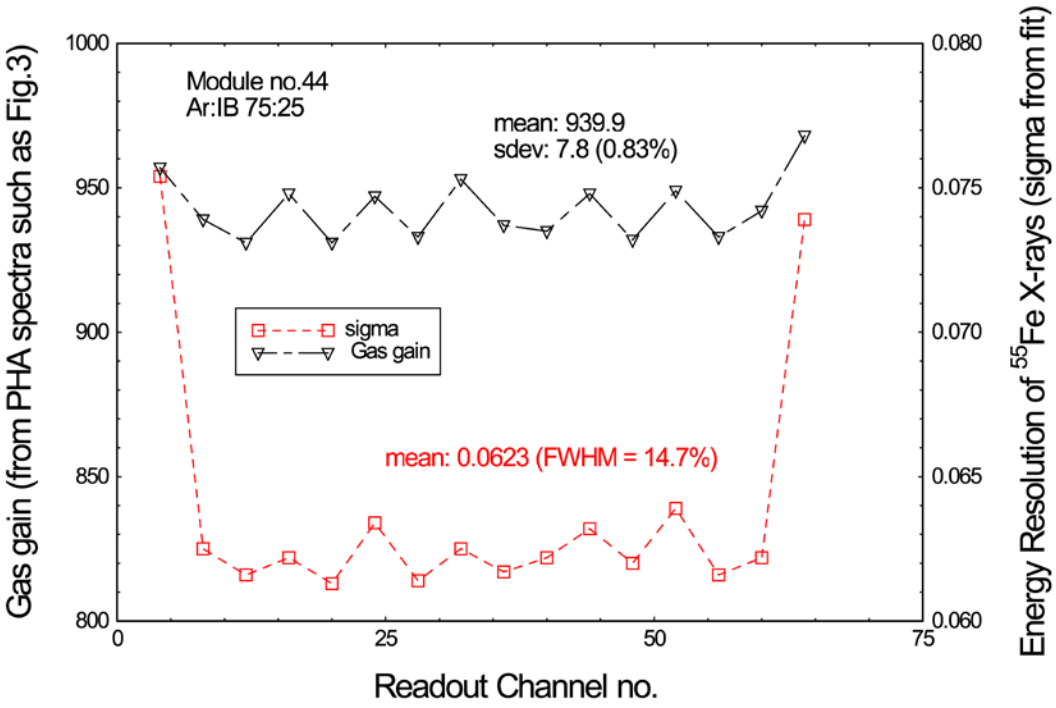

Figure 5: Variation of gas gain and energy resolution across module no.44

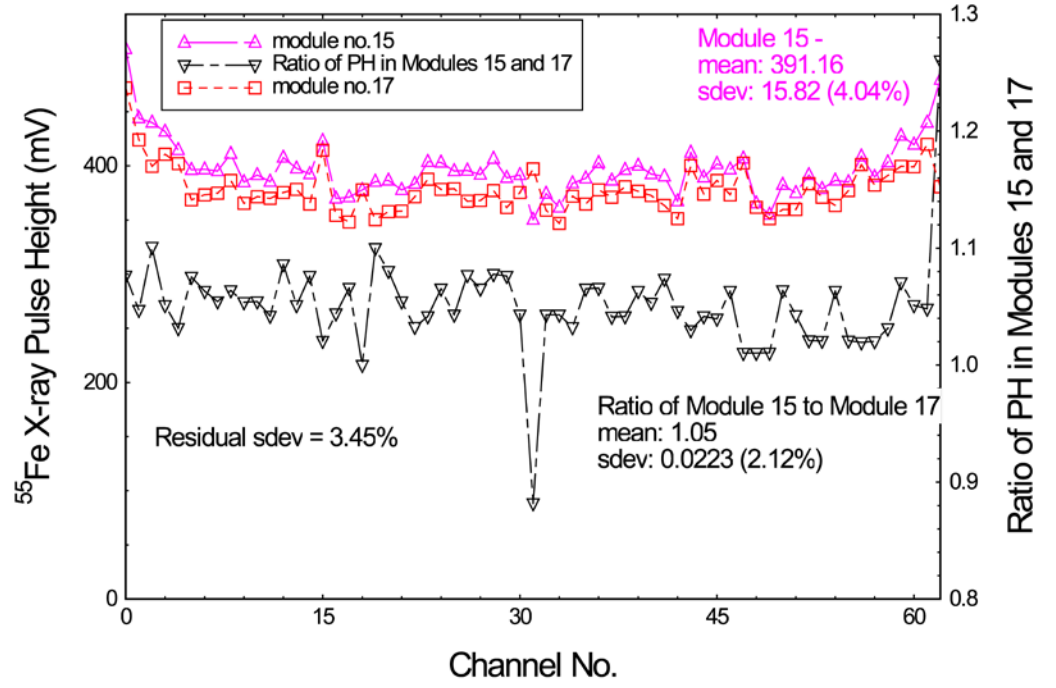

Figure 6: Comparison of the individual channel pulse heights from two modules using the 16 channel preamp readout.

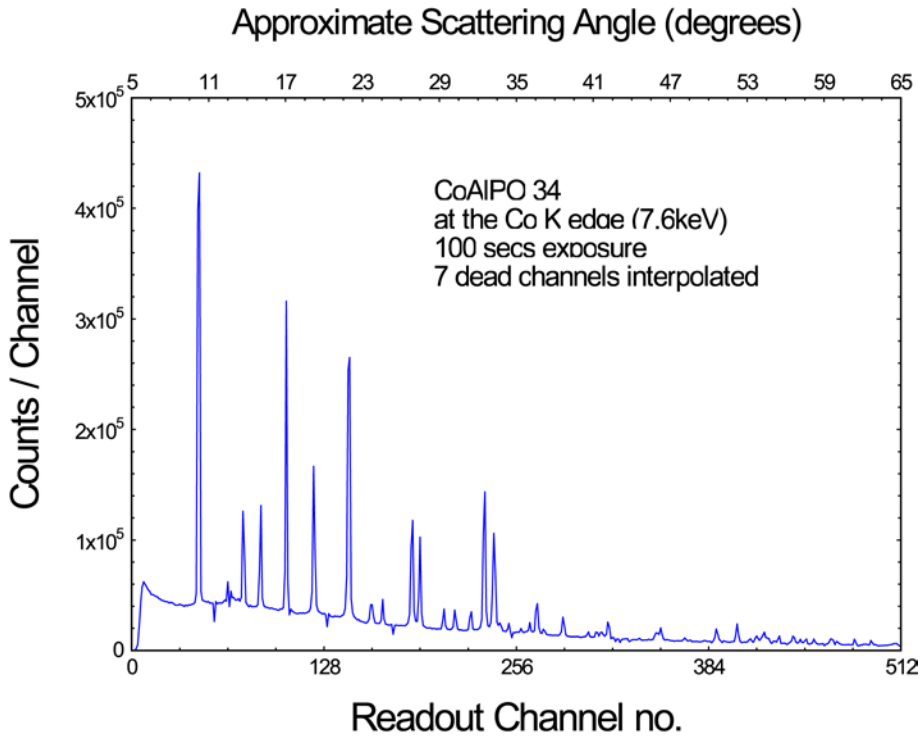

Figure 7: HOTWAXS scattering spectrum of a CoAlPO 34 sample on station 9.3.
(100 seconds exposure)

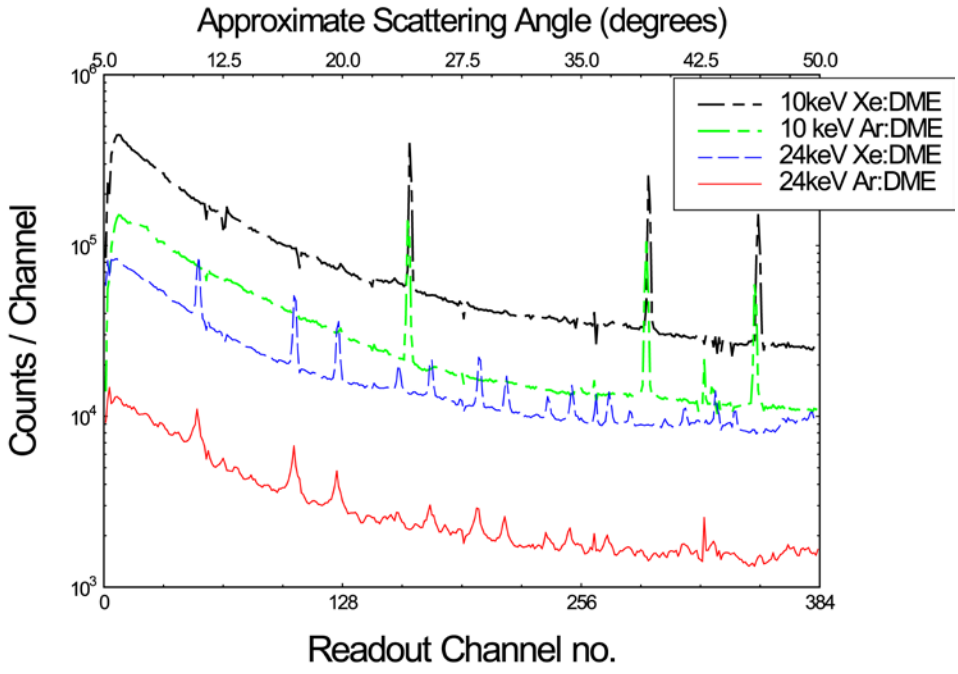

Figure 8: Silicon diffraction patterns measured at stated X-ray energies.
for Ar:DME and Xe:DME gas mixtures

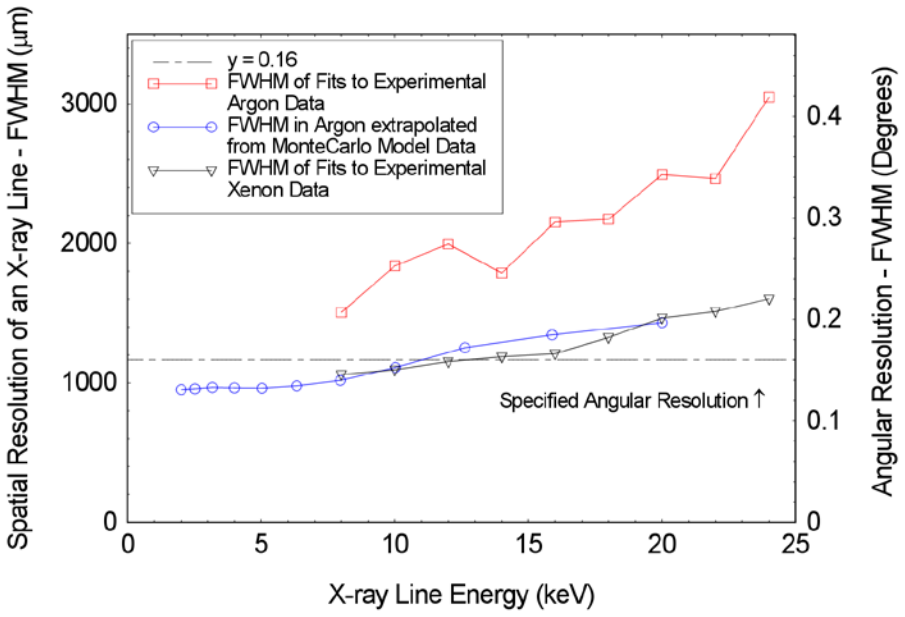

Figure 9: Variation of spatial (angular) resolution with X-ray energy with argon and xenon gas mixtures

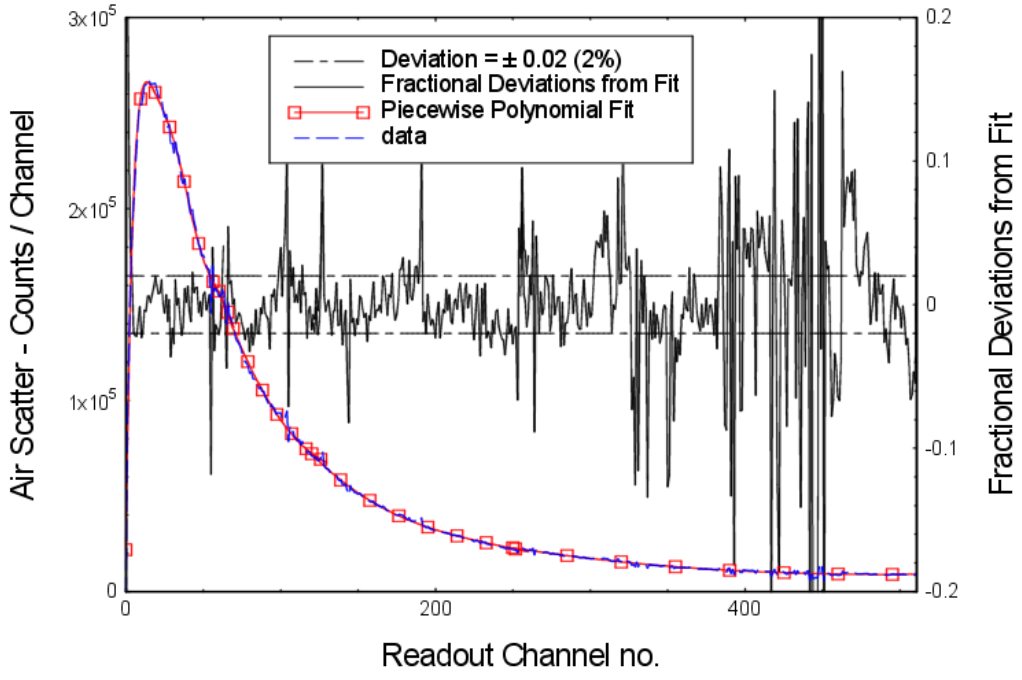

Figure 10: Air scatter response of HOTWAXS with polynomial fit.

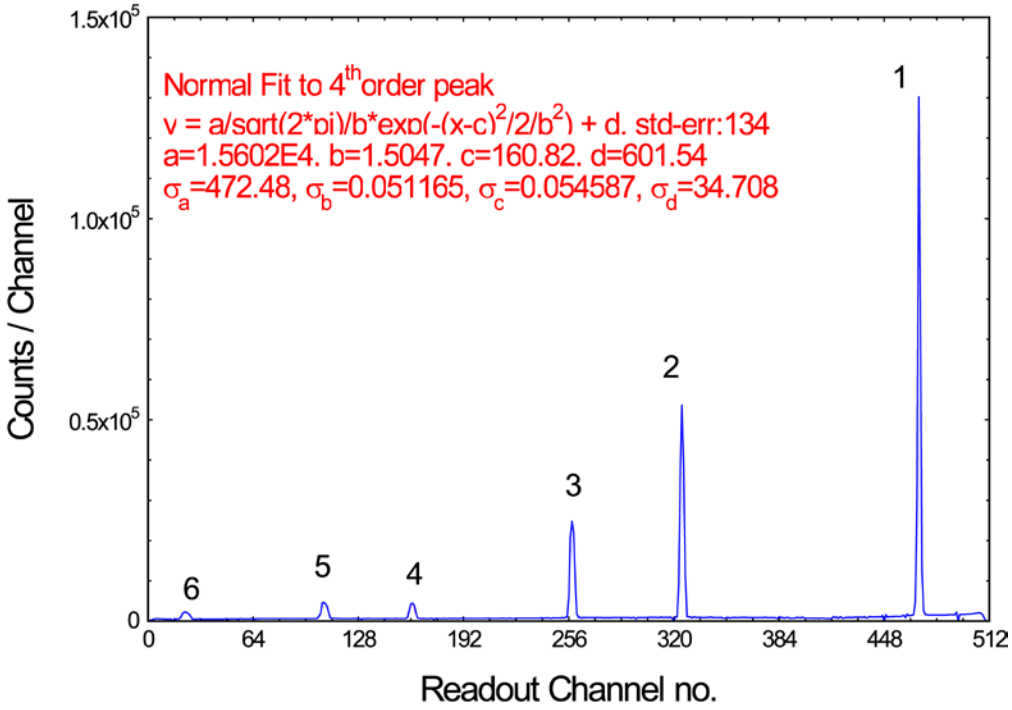

Figure 11: HOTWAXS silicon diffraction data from station 16.1

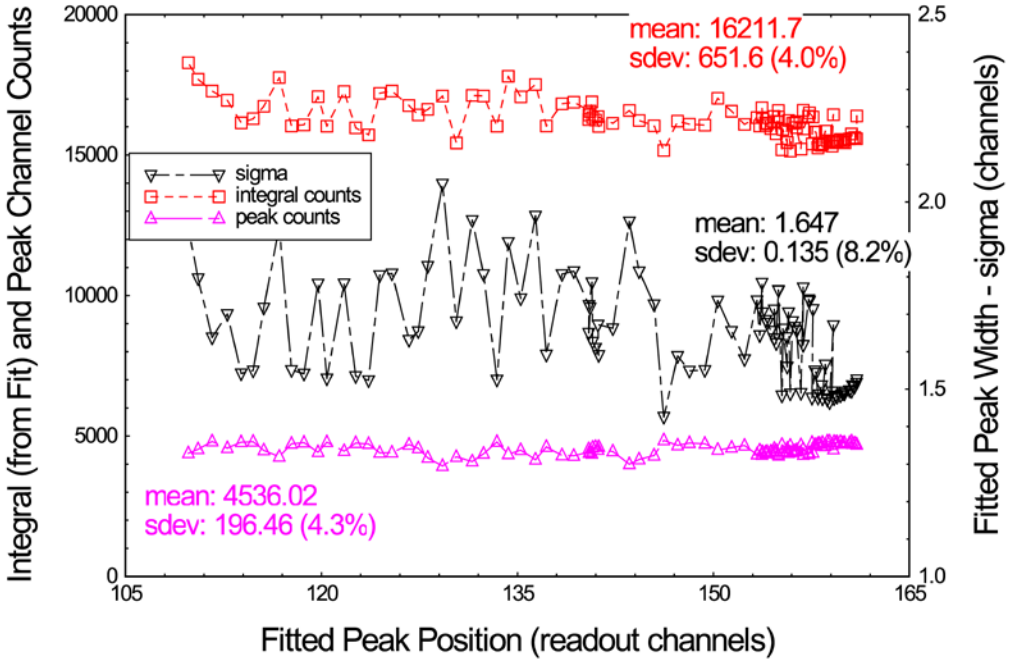

Figure 12: Variation of integral counts, peak counts and line resolution (Gaussian Fits) for 4th order Si peak of Figure 11

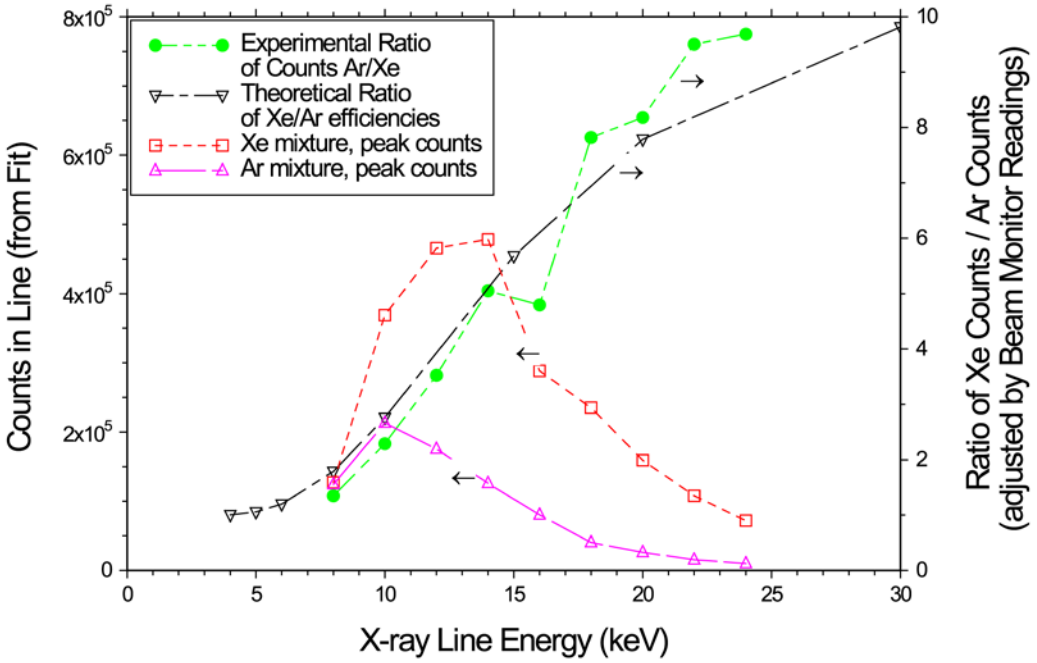

Figure 13: Energy response curves of HOTWAXS for each of the gas mixtures

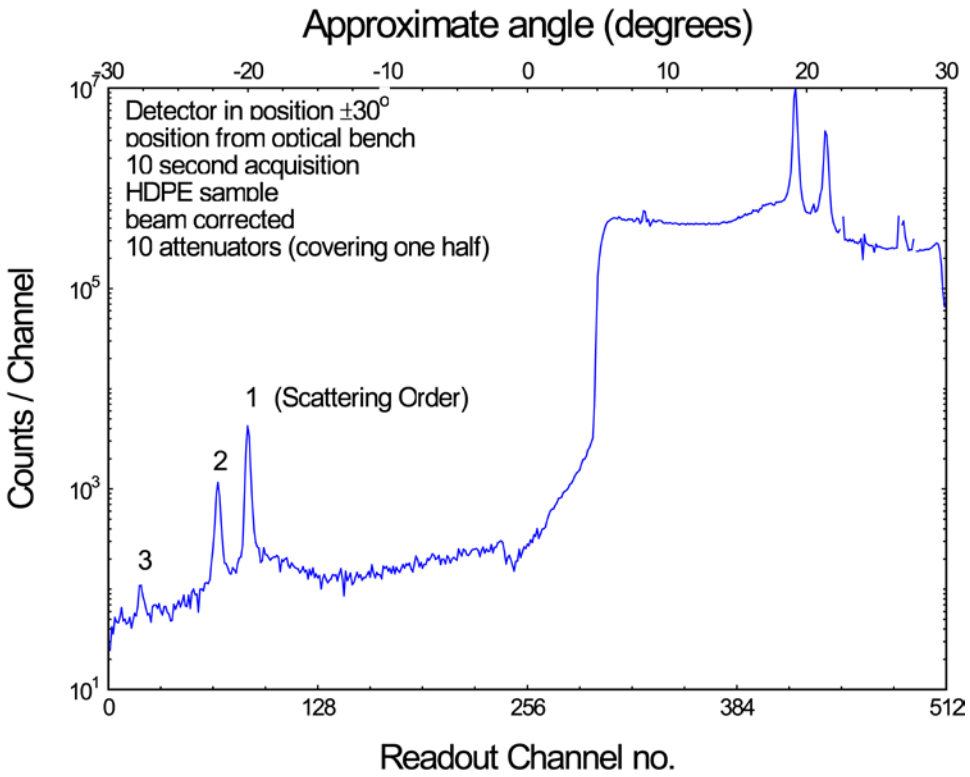

Figure 14: HDPE scattering data with 10 attenuators covering half of the detector

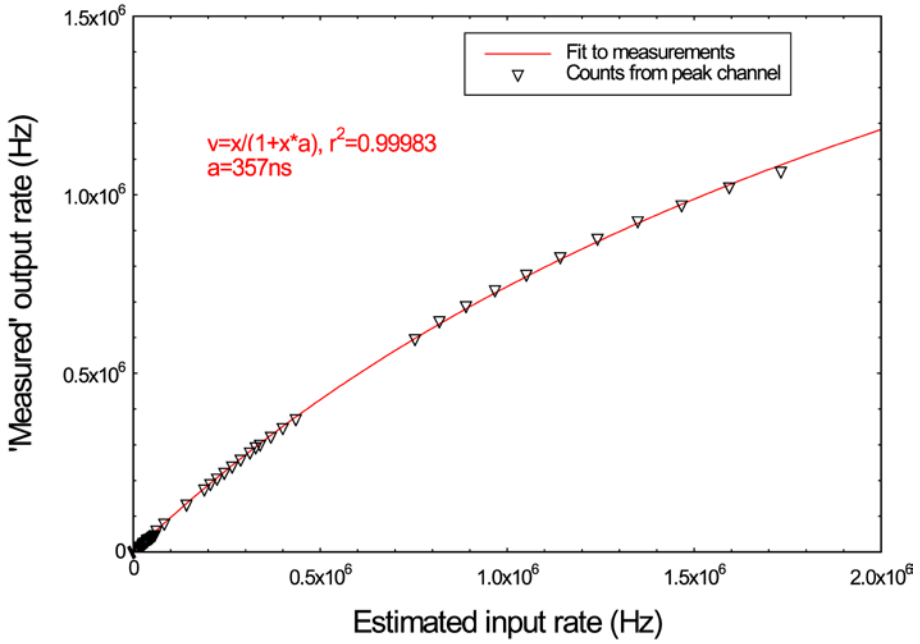

Figure 15: Measured deadtime calibration for the HOTWAXS detector

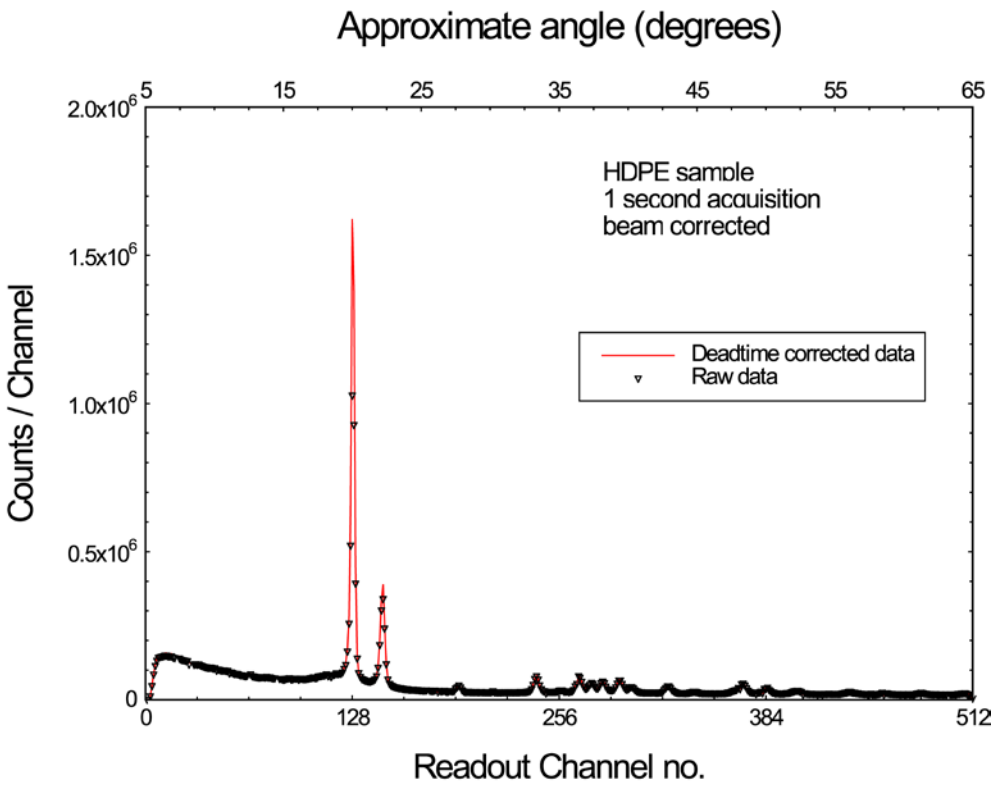

Figure 16: 1 second exposure with HDPE in beam showing raw and deadtime-corrected data.

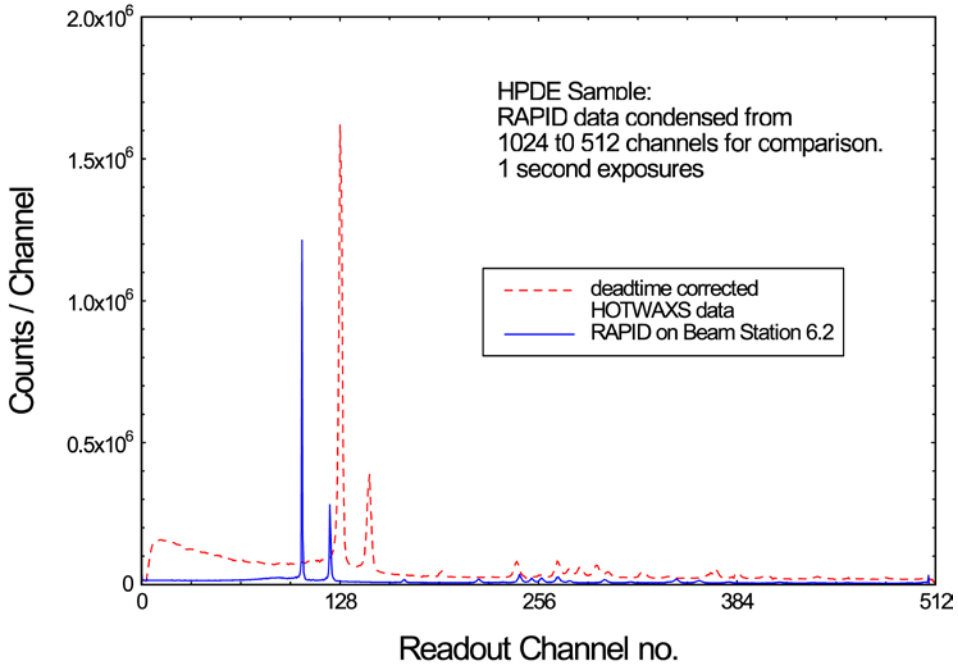

Figure 17: Comparison of deadtime corrected HDPE data from HOTWAXS with RAPID2 data.

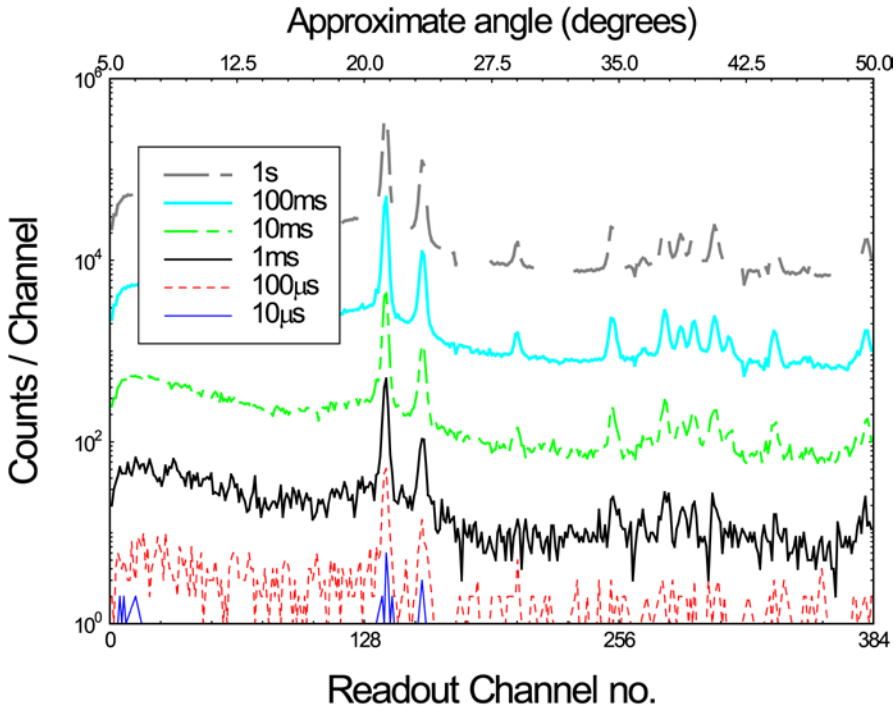

Figure 18: HDPE diffraction data measured in decreasing time frame periods.

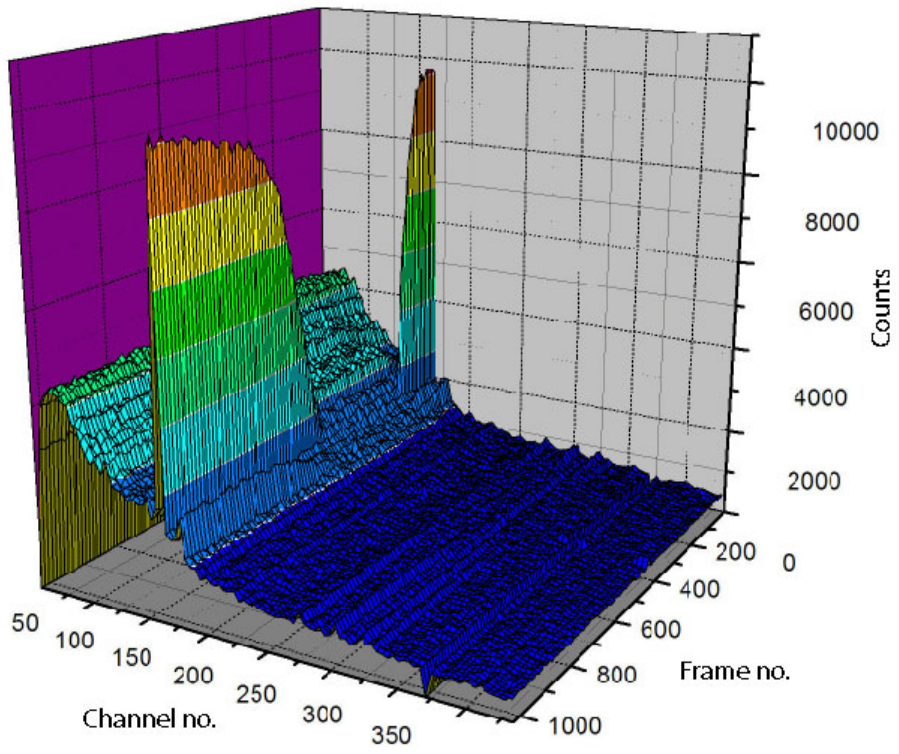

Figure 19: 3D representation of the melting and re-crystallisation of HDPE, only 128 frames shown for clarity.